

Review

Azobenzenes and heteroaromatic nitrogen cyclopalladated complexes for advanced applications

Mauro Ghedini*, Iolinda Aiello, Alessandra Crispini, Attilio Golemme,
Massimo La Deda, Daniela Pucci

*Centro di Eccellenza CEMIF.CAL and LASCAMM, CR-INSTM, Unità INSTM della Calabria, Dipartimento di Chimica,
Università della Calabria, I-87036 Arcavacata (CS), Italy*

Received 30 July 2005; accepted 9 December 2005

Available online 18 January 2006

Contents

1. Introduction	1373
2. The cyclopalladated ring	1374
2.1. Background	1374
2.2. Electronic conjugation and metalloaromaticity	1375
2.3. Intermolecular interactions	1376
3. Important physical properties	1376
3.1. Thermotropic mesomorphism	1376
3.2. Photoconduction	1377
3.3. Photorefractivity	1377
4. Classes of cyclopalladated materials	1378
4.1. Dinuclear [(C,N)Pd(μ-X)] ₂ complexes	1378
4.2. Mononuclear (C,N)Pd(O,N)	1381
4.3. Mononuclear (C,N)Pd(O,O)	1385
4.4. Mononuclear (C,N)Pd(N,N)	1386
5. Conclusions and perspectives	1387
5.1. Synthesis of new species with improved performances	1387
5.2. Further applications	1388
Acknowledgements	1389
References	1389

Abstract

The five-membered “(C,N)Pd” metallacycle is a structural feature common to a number of stable photoactive molecular materials. This review is centred on the connection among molecular geometries, types of ligand and photophysical, optical, thermal and electrooptical properties of several series of dinuclear and mononuclear cyclopalladated species, based on HC₂N ligands (HC₂N = azobenzenes or nitrogen containing heteroaromatic ligands). In the discussion, some representative examples of complexes featuring an useful set of physical properties, were selected and divided into different classes, depending on the nature of the ancillary ligands bonded to the “(C,N)Pd” fragment.

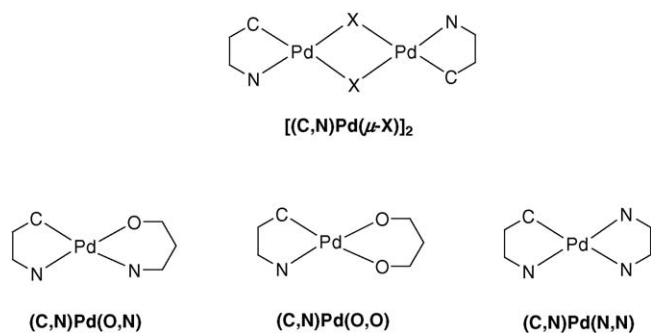
© 2005 Elsevier B.V. All rights reserved.

Keywords: Cyclopalladated complexes; Molecular materials; Liquid crystals; Luminescence; Photoconductivity; Photorefractivity

1. Introduction

The very rich palladium(II) chemistry includes elusive species, often invoked to explain intriguing catalytic processes, reactive precursors involved in important chemical syntheses,

* Corresponding author. Tel.: +39 0984 492062; fax: +39 0984 482066.
E-mail address: m.ghedini@unical.it (M. Ghedini).



Scheme 1. Schematic representation of four main topological classes of five-membered palladacycles with different complementary ligands.

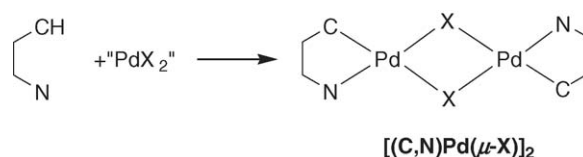
and inert and stable compounds used as materials for many applications spanning from photonics to biochemistry, as shown by the recent comprehensive reviews [1]. The “(C,N)Pd” metallacycle is a structural feature with very high stability and the formation of cyclopalladated complexes is an extensively investigated subject. Moving within the realm of cyclopalladated species, as mesomorphism and related properties have already been extensively reported [1b], the aim of this review, is to document the thermotropic photoconductive, photorefractive and luminescent properties of cyclopalladated complexes formed by azobenzenes or nitrogen containing heteroaromatic ligands, in order to show how appropriate synthetic paths can make new multifunctional materials available.

Metal coordination of organic ligands provides a new concept for the synthesis of “non-conventional” systems, with chemical and physical properties modulated by the contribution of different and tunable synthons: the metal–ligand cyclometalated fragment as a central unit, the flexible chains, variable in size and number, at the periphery and the many different types of complementary ligands which complete the coordination sphere of the palladium(II) ion. As the physical properties these materials are expected to display are strongly related to the peculiar structural and electronic nature of the five-membered “(C,N)Pd” metallacycle, in the present survey some features of such a molecular fragment will be preliminarily discussed. Thereafter, a brief introduction to thermotropic mesomorphism, photoconductivity and photorefractivity will be given. For the sake of conciseness, in the context of this contribution, only palladium(II) derivatives of azo and azoxybenzenes, benzo[*h*]quinoline, phenyl-pyridines and phenyl-pyrimidines (in the following generally indicated as HC,N) will be considered, i.e., only those with planar five-membered palladacycles. Four main topological classes different in their complementary ligands and/or geometrical shape will be reviewed, namely $[(C,N)Pd(\mu-X)]_2$, $(C,N)Pd(O,N)$, $(C,N)Pd(O,O)$ and $(C,N)Pd(N,N)$ (Scheme 1) emphasizing for each class, the distinguishing physical features.

2. The cyclopalladated ring

2.1. Background

The chemistry of cyclopalladated complexes is a very fascinating and popular subject in constant evolution, as shown by



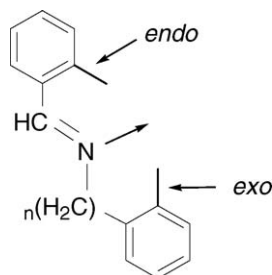
Scheme 2. Scheme of a cyclopalladation reaction and formation of five-membered cyclopalladated rings.

the recent publication of comprehensive reviews [1]. For this reason, the basic concepts dealing with synthesis and reactivity, usually extensively discussed, will not be described in this work, which will instead focus on different features of the “(C,N)Pd” containing species considered as molecular materials.

Cyclopalladation is generally considered as a two-step reaction, which involves one ligating group holding the metal centre close to a C–H bond and the subsequent closure of the ring via the formation of the carbon to metal bond [1]. The definition of σ -bond formation as electrophilic substitution has been obtained from studies conducted on palladium(II) azobenzene derivatives, where cyclopalladation (Scheme 2) occurs on the benzene ring bearing electron donating substituents [2].

N-donor substrates such as azobenzenes, imines, phenylpyridine and benzo[*h*]quinoline have been extensively used in cyclometallation reactions and have shown a strong tendency to form, with palladium precursors, cyclopalladated five-membered rings containing square-planar palladium(II) centres. The stability of the resulting metal-containing ring is the reason motivating several investigations of the mechanisms of important catalytic processes, since it can be regarded as a possible intermediate in metal-catalyzed C–H bond activation. Moreover, considering the facility of formation of five-membered compounds through cyclometallation reactions, cyclometalated complexes are utilized as intermediates for organic synthesis, and excellent reviews on their applications have recently appeared [1,3–5].

The discussion about the predominance of the formation and the stability of cyclometalated compounds containing five-membered rings started long ago, when it was established that ligands capable of forming five-membered metal chelate rings lead to the most stable products. Some important differences exist within the large number of complexes containing five-membered rings, originating from the differences in the nature and in the geometry of the coordinating ligands, which could be responsible for the significantly different properties of the resulting materials. The catalytic properties of cyclopalladated complexes can be taken as an example, since they depend on the type of palladacycle present in the structure. In fact, the majority of palladacycles are reactive towards a wide number of reagents used in catalysis and, in these cases, reduction of Pd(II) to Pd(0) occurs. In other cases, palladacycles are instead recovered unchanged following catalysis and can therefore be recycled, such as in the case of a series of palladium imine complexes, in which the metal centre is stabilized by a five-membered planar ring containing an sp^2 -hybridized nitrogen atom [6].

Scheme 3. *Endo* and *exo* metallacycles in *N*-benzyl-benzylidene-amines.

2.2. Electronic conjugation and metalloaromaticity

The existence of a certain level of “aromaticity” in five-membered rings, involving two conjugated double bonds ($C=N-C=C$) and the filled palladium d orbitals of appropriate symmetry, has been proposed for the first time by Crociani et al. in order to explain IR spectra of endocyclic complexes [7]. Since then, there has been some debate over the role of electron delocalization within the metallacycle as a driving force towards cyclization reactions. As an example, *N*-benzyl-benzylidene-amines have been used to obtain, through the development of many synthetic methods of preparation, both *endo* and *exo* metallacycles (Scheme 3). The main and important difference between the *endo* and *exo* structural isomers is the presence of the carbon nitrogen double bond inside or outside the metallacycle, respectively [8]. The study of the mechanism of the cyclopalladation reactions in these systems and of their applications in organic synthesis have been the subject of a significant number of papers [9–11]. A possible explanation for the strong preference for the formation of the *endo* isomers is the stabilization due to a partial electron delocalization within the five-membered ring, and therefore a certain degree of aromatic character.

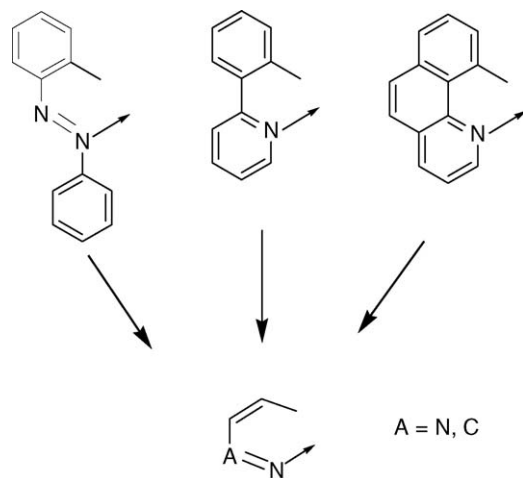
Metalloaromaticity, that is the manifestation of aromatic properties in chelate metallacycles, was first described by Calvin and Wilson in 1945 to explain the stability of β -diketonate copper(II) complexes [12]. Since then, there has been a growing interest in the recognition of metalloaromatics as important intermediates in reactions catalyzed by organometallic compounds. A recent review has outlined the importance of metalloaromaticity as a unifying concept between molecular structures and properties, and has pointed out the general criteria to assess aromaticity. The criteria have been broadly divided into three categories: resonance energy stabilization, spectral and/or magnetic measurements and various molecular structure parameters [13]. Since metalloaromaticity affects bond orders and geometrical parameters within the cycles, aromaticity indices based on experimental bond lengths, typically used in the analysis of five or six-membered organic heterocycles, have also been considered in the analysis of the “aromatic” character of five-membered cyclopalladated rings [14]. In particular, the harmonic oscillator model of aromaticity (HOMA) has been applied to the study of the delocalization in five-membered cyclopalladated systems with the intention of establishing a correlation between the structural evidences of aromaticity (such as planarity) and aromaticity indices predominantly used

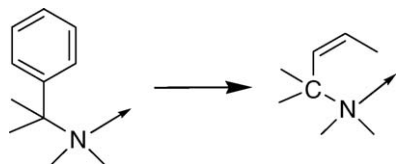
N=N 1.25	1.27 Å	C=N 1.35	1.36 Å
C-C 1.43	1.40	C-C 1.48	1.46
C=C 1.39	1.41	C=C 1.39	1.41

Scheme 4. Variation of the C–C, N–C and N–N bond lengths in free ligands and in their corresponding PdNNCC and PdNCCC metallacycles.

in organic chemistry. The HOMA index is based on the bond lengths and bond orders within the metallacycle, and their variations compared to the uncoordinated ligands. In fact, a preliminary analysis of the C–C, N–C and N–N bond lengths in both the unmetallated and metallated ligands within the metallacycle has been performed using Cambridge Structural Database (CSD). Preliminary results showed that in the case of PdNNCC and PdNCCC palladacycles, there is a slight variation in the alternation of lengthening and shortening of the bond distances within the metallocycle (Scheme 4).

The search has been restricted to planar palladacycles obtained through palladation species where the $C=N$ or the $N=N$ bonds are within the cycle. The results of these studies confirm, as expected, that deviation from planarity in cyclopalladated rings is related to the hybridization of the N atom, indicating that planarity can be assumed to be an important condition for “aromaticity”. When the five-membered cyclopalladated ring belongs to complexes containing azobenzene, phenylpyridine or benzo[*h*]quinoline (Scheme 5) as chelate ligands, the presence of an sp^2 -hybridized N atom within the ring assures planarity of the molecular fragment. Aromaticity indices allow then a quantitative estimate of how much the breaking of planarity of the π electron system decreases its aromatic character.

Scheme 5. Planar five-membered palladacycles generated from chelation of azobenzene, 2-phenylpyridine and benzo[*h*]quinoline ligands.



Scheme 6. Non-planar and non-aromatic metallacycles obtained through chelation of amine ligands.

The difference in the aromatic character of five-membered cyclopalladated rings is reflected in a different reactivity of the whole system. The sequence of increasing “aromaticity” of the cyclopalladated compounds obtained through the described molecular structure parameters approach, is the same as the decreasing reactivity sequence obtained from studies of ligand-exchange reactions: complexes containing amine ligands (Scheme 6) and therefore non-planar and non-aromatic metallacycles, show the highest reactivity [15].

2.3. Intermolecular interactions

New structural evidence of metalloaromaticity is given by the existence of π – π stacking interactions with average distance of 3.4 Å, generated by metal chelated rings. An interesting example has been reported recently in the case of a copper(II) 1,10-phenanthroline derivative in which the metallacycle of the N,N type is involved in an intramolecular effective “metal chelate ring/aromatic ring” π – π stacking interaction [16]. Examples of metallacycles of the C,N type, that is cyclometalated rings, that contribute to π – π stacking interactions within the molecular arrangement, are given by the cyclopalladated phenylhydrazone complexes [17]. The 2-benzoylpyridine-*N*-methyl-*N*-phenylhydrazone coordinated to a “PdCl” fragment (Fig. 1) is just one of the many reported examples that prove how the presence of fused rings formed by the palladacycle and the palladated phenyl ring induces planarity and, to some extent, electron

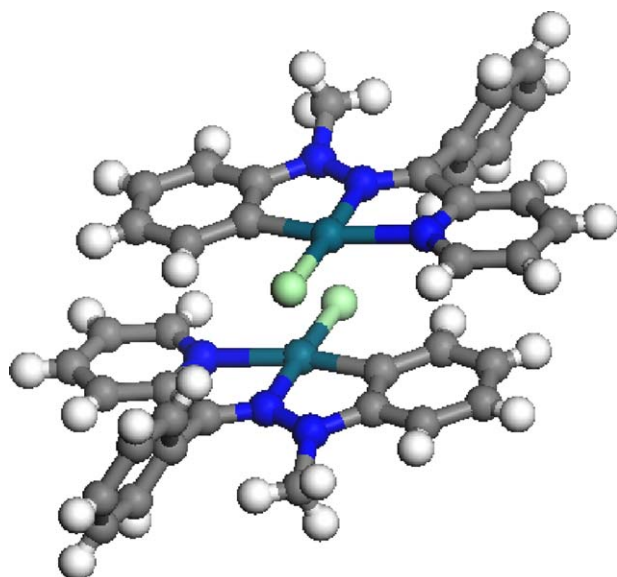


Fig. 1. A view of the interaction between planar aromatic fused rings of molecules of 2-benzoylpyridine-*N*-methyl-*N*-phenylhydrazone Pd(II) complex.

delocalization. The photophysical characterization of these complexes has pointed out the importance of the intermolecular interactions involving aromatic rings for the appearance of luminescence [17], very unusual in palladium(II) complexes, in the crystalline state at room temperature. These examples show the important role of electron delocalization on various properties of cyclopalladated complexes as molecular materials.

3. Important physical properties

3.1. Thermotropic mesomorphism

The liquid crystalline state occurs as one or more intermediate phases (mesophases) between the melting point (crystal-mesophase transition) and the clearing point (mesophase-isotropic liquid transition) [18]. Thermotropic liquid crystals are traditionally grouped in two main classes according to the structural motif of the constituent molecules (Fig. 2), namely calamitic or rod-like (molecules with an elongated rigid core and for which a molecular axis is much longer than the other two) and discotic or disk-like (where one molecular axis is much shorter than the other two).

Different mesophases are classified according to the different molecular orientational and positional order exhibited, as shown in Fig. 2. In the least ordered mesophase, called nematic, long-range orientational order is present, while positional order is only short-range, as in isotropic liquids: the only ordering consists in the average parallel alignment of molecules in one common direction, identified by a versor (director). Both rod-like and disk-like molecules can originate nematic phases, called N and N_D, respectively. Mesophases exhibiting, in addition to orientational order, also a certain degree of positional order, are called smectic phases, Sm in short. In the smectic state, molecules tend to be arranged within layers or planes. Considering possible correlations within the layers and between the layers, there are five true smectic modifications and a further six quasi-smectic disordered crystal mesophases. The quasi-smectic crystal phases are indicated by the letters B, J, G and E, K, H while the true

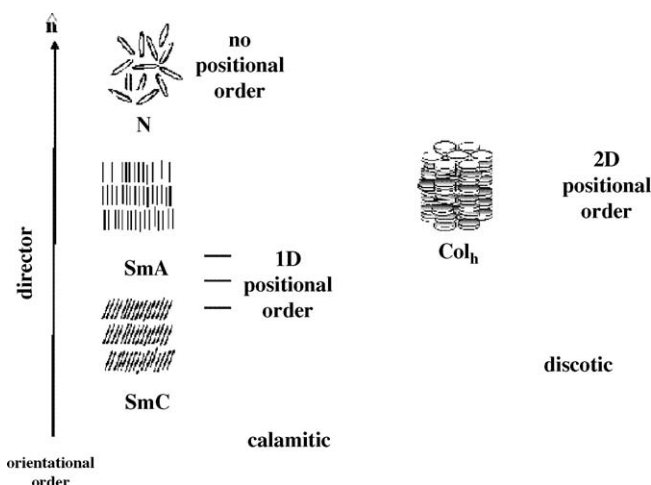


Fig. 2. Schematic representation of the molecular arrangement in some mesophases.

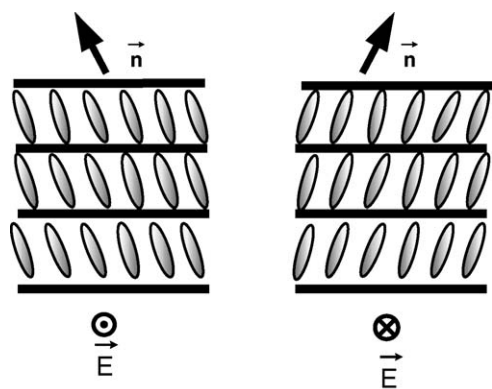


Fig. 3. Illustration of the electric field induced reorientation of the director in a SmC* phase.

smectic liquid crystals by the symbol Sm followed by a letter for the phase type (SmA, SmC, SmB, SmI and SmF). The least ordered smectic liquid crystal phases are the SmA and its tilted analogue SmC (Fig. 2).

One of the most important smectic phases from a technological point of view is the chiral smectic C phase (SmC*). The peculiar feature of this mesophase is that it is intrinsically ferroelectric, with a spontaneous polarization within the smectic layers which is coupled to a tilt of the average molecular orientation with respect to the layer normal, as schematically illustrated in Fig. 3. The polarization, and the tilt angle, can be rapidly reoriented by an applied field, with typical switching times in the hundreds of microseconds, or even lower.

Columnar discotic phases are the equivalent of the smectic phases for calamitic liquid crystals. In columnar phases molecular cores are aligned in columns, which are surrounded by side chains and can be arranged in various ways, as for example, in hexagonal or rectangular lattices.

The thermotropic mesomorphism of liquid crystalline materials is detected and investigated combining different techniques: polarized optical microscopy (POM) for the textures, differential scanning calorimetry (DSC) for the phase transitions and powered X-ray diffraction (PXRD) variable temperature for the molecular positional and orientational order.

3.2. Photoconduction

Photoconduction requires two main properties. The first one is that light absorption must be followed by a process during which a “free” electron and a “free” hole are generated. In this context “free” means that they are separated by a distance which is large enough for the Coulomb attraction to be smaller than thermal energy. The second requirement is that the generated charges must be able to diffuse, or drift, through the material. How well a substance photoconducts depends then on absorption coefficients, quantum efficiency of carrier generation and carrier mobility. Models to describe both photogeneration and mobility have been developed at first for inorganic crystalline materials [19] where a band structure can be considered for the electronic energies. Because of the relative lack of complexity of such models, they have often been applied to describe the same

properties in molecular amorphous materials, where electrons states are localized. This is still common, albeit questionable, practice since the models more recently developed for amorphous organics [20–22] include a certain number parameters often unknown or difficult to measure. In any case, the different models describe, with more or less accuracy, experimental evidence that shows how charge generation is field assisted, with a quantum efficiency increasing with the applied electric field, while mobilities exhibit a more complicated field dependence. In particular, carrier mobility is generally attributed to a hopping mechanism between localized molecular states, corresponding to a series of oxidations or reductions of the neutral molecule for hole or electron conduction, respectively.

Photoconductivity is measured by monitoring the voltage drop across a resistor (which must be much smaller than the voltage drop across the sample) in series with the sample. The current flowing through the circuit is then measured with and without illumination and the difference is considered as the photocurrent. In order to compare among different samples, photoconductivity may be normalized with respect to light intensity (power per unit surface) and absorption coefficient.

3.3. Photorefractivity

When a photoconductor is illuminated with a non-uniform light pattern, due to the different mobilities of electrons and holes, a non-uniform charge distribution and the resulting space-charge electric field are established. In addition, if the refractive index of the material is field-dependent, an index replica of the light pattern is obtained. Depending on the nature of the material, these holograms can be permanent or not and can be used for a variety of applications ranging from holographic memories to image treatment and medical imaging. Although several different physical mechanisms might be at the origin of light-induced refractive index variations, the photorefractive one is unique because the resulting index hologram is phase shifted with respect to the generating light pattern, a feature that can be used in a number of applications.

Photorefractive performance is conveniently monitored by following the diffraction properties of a grating obtained by illuminating samples with the interference fringes generated by two overlapping coherent laser beams. Electric fields are always applied when such measurements are carried out on organic materials, since photogeneration efficiency in this case is strongly enhanced. In addition, in order to induce a drift component along the grating wavevector, samples (in the form of films, with a thickness between 3 and 100 μm , usually between transparent conducting glass slides) are tilted so that their normal and the bisector of the incoming laser beams are not collinear. If the mechanism of grating formation is photorefractive, then the resulting refractive index pattern will be phase shifted with respect to the interference fringes, producing an energy exchange between the laser beams. This intensity exchange is quantified by a gain coefficient Γ , defined as:

$$\Gamma = \frac{2\pi}{\lambda \Delta n \sin \theta} \quad (1)$$

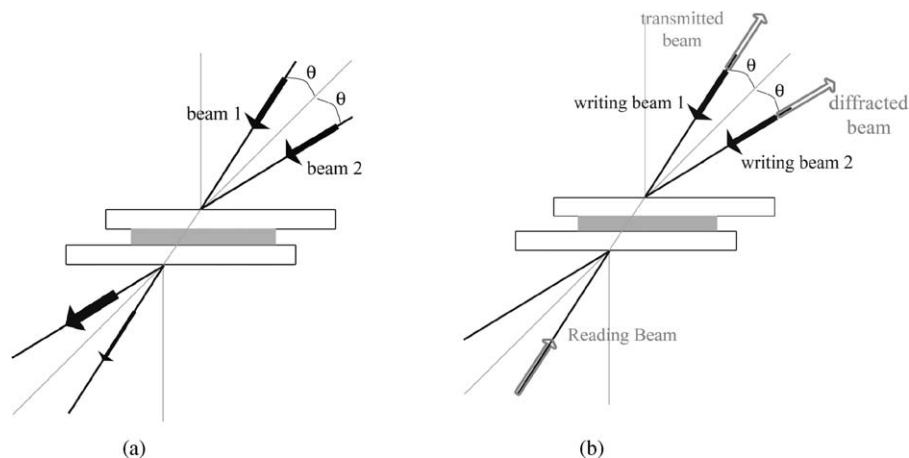


Fig. 4. Schematic illustration of the multi-wave mixing experiments used to characterize photorefractive performance. Samples are usually placed between two conducting glass slides and illuminated with two overlapping coherent light beams. In two-beam coupling experiments (a) the energy exchange between the two beams is recorded, as a function of time or of applied electric field. In four-wave mixing (b) a third beam, which can be partially diffracted, probes the resulting photorefractive index grating.

where λ is the light wavelength, Δn the refractive index modulation amplitude and θ is the above mentioned phase shift. The Γ value can be experimentally obtained by considering each beam intensity with and without the other beam turned on:

$$\Gamma = \frac{1}{d_1} \ln \frac{I_1(I_2 \neq 0)}{I_1(I_2 = 0)} - \frac{1}{d_2} \ln \frac{I_2(I_1 \neq 0)}{I_2(I_1 = 0)} \quad (2)$$

where d_1 and d_2 are the path lengths of beams 1 and 2 in the sample and $I_1(I_2 \neq 0)$ and $I_1(I_2 = 0)$ are the intensities of beam 1 beyond the sample with beam 2 on and off, respectively. Similar definitions apply to $I_2(I_1 \neq 0)$ and $I_2(I_1 = 0)$. The observation of energy exchange in thick gratings is generally taken as the final experimental evidence for the non-local (i.e., photorefractive) nature of the grating. Fig. 4(a) includes a schematic illustration of this two-beam coupling (2BC) experiment.

Photorefractive gratings can also be characterized, as with all gratings, by measuring their diffraction efficiency η . For thick gratings (i.e., in the Bragg regime) the efficiency is measured, as illustrated in Fig. 4(b), in four-wave mixing geometries.

In this case, a third “reading” laser beam, usually of the same wavelength of the other two “writing” beams, is used to probe the resulting grating: the diffraction efficiency of the grating is defined as the diffracted fraction of the reading beam intensity. In the case of thin gratings (i.e., in the Raman–Nath regime) when multiple diffraction orders are observed, diffraction efficiency is usually defined as the intensity of the first order diffraction normalized to the intensity of the corresponding writing beam before diffraction.

Electric field induced refractive index variations can be monitored in ellipsometric measurements. In this case, the sample is placed between crossed polarizers along the path of a single light beam. If the sample is tilted with respect to the beam, when the application of a dc electric field will induce a refractive index variation, the sample will act as a phase retarder and a certain amount of light, proportional to the index variation, will pass through the second polarizer. Similar experiments can be carried out by using biased ac electric fields. In this

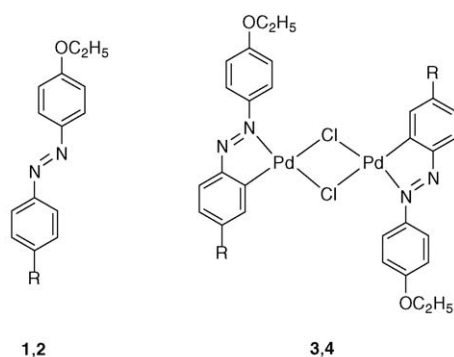
case a compensator (variable phase retardation plate) is often placed right after the sample to increase sensitivity. The variation of the transmitted light intensity at the same frequency of the applied field is then followed, often by using a lock-in amplifier. These experiments are useful to check the speed of the field-induced index modulation: during a frequency sweep, slow physical mechanisms will gradually become inactive at higher frequencies.

4. Classes of cyclopalladated materials

4.1. Dinuclear $[(C,N)Pd(\mu-X)]_2$ complexes

Cyclopalladated complexes are obtained through a reaction of a palladium(II) precursor, usually M_2PdCl_4 ($M = Li$ or K), $Pd(OAc)_2$ or $(PhCN)_2PdCl_2$, with a selected organic substrate bearing a planar sp^2 nitrogen atom three chemical bonds from an aromatic C–H fragment. The resulting product is a bimetallic species in which two “(C,N)PdX” halves are mutually joined by the anions X ($X = Cl$ or AcO). This reaction can also be considered as the first step of more complex syntheses and that, from a synthetic point of view, a dinuclear $[(C,N)Pd(\mu-X)]_2$ complex is therefore the parent of all species containing the same cyclopalladated HC,N ligand.

Among different important properties of the dinuclear complexes, mesogenic behaviour hold a relevant position. The considerations that azobenzenes, disubstituted at the p,p'-positions with linear aliphatic chains, are well known rod-like thermotropic liquid crystalline compounds [23] and at the same time can act as ligands in cyclopalladation reactions prompted us to undertake investigations on a new class of materials: organometallic liquid crystals [24], successively named metal-lomesogens by Giroud-Godquin and Maitlis [25]. The products of these first attempts were nematic palladiomesogens that, when compared to the liquid crystalline ligands, exhibited a thermal behaviour with higher phase transition temperatures and reduced mesophase temperature range (Scheme 7).



Compound	R	Mesomorphism		
1	C ₆ H ₁₃ COO	C 59 °C	N 112 °C	I
2	CH ₂ =CH(CH ₂) ₈ COO	C 64 °C	N 107 °C	I
3	C ₆ H ₁₃ COO	C 190 °C	N 205 °C	I
4	CH ₂ =CH(CH ₂) ₈ COO	C 165 °C	N 185 °C	I

Scheme 7. Mesogenic behaviour of representative examples of 4,4'-disubstituted-azobenzene ligands and of the corresponding chloro-bridged dinuclear complexes.

Single crystal X-ray structure determinations of similar dinuclear palladium(II) complexes containing cyclometalated azobenzenes (e.g., X-ray structure of di- μ -chloro-bis[(4-hydroxy-4'-methylazobenzenato- C^2, N^2)palladium(II)]; Fig. 5), showed the overall “H-shaped” molecular structure of these systems, in which the “(C,N)Pd” chelate rings are essentially coplanar and the two azo-ligands are joined through central bridged groups [26].

Molecular order within the mesophases and transition temperatures were found [27] to depend on the nature of the bridging halide (Scheme 8) and in order to stress the role of the X bridge on

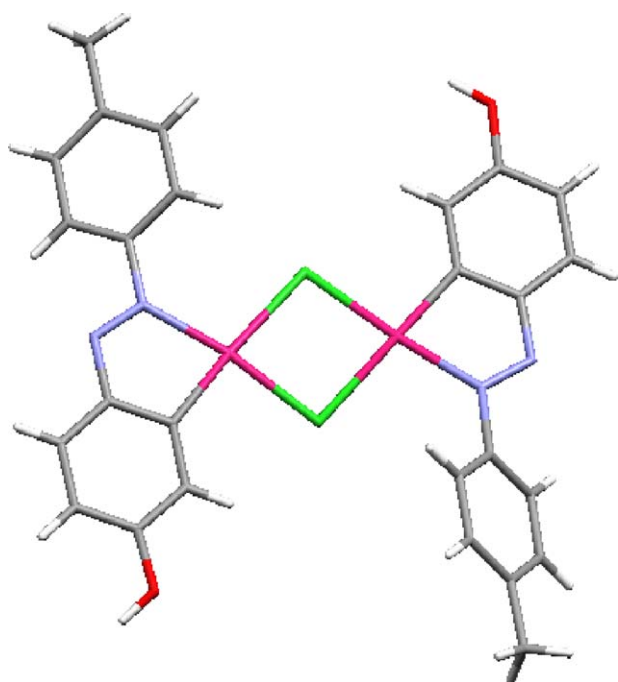
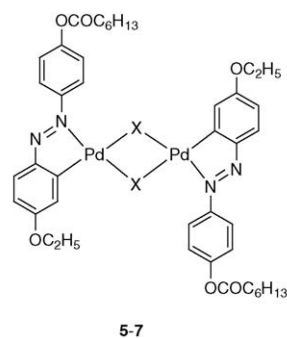


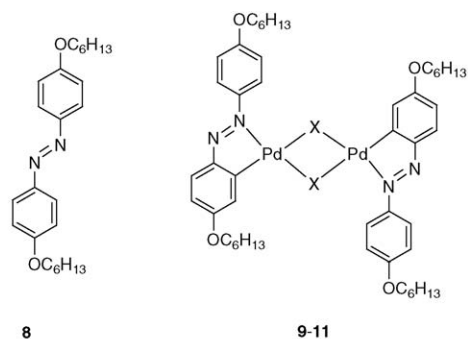
Fig. 5. H-shaped molecular structure of di- μ -chloro-bis[(4-hydroxy-4'-methylazobenzenato- C^2, N^2)palladium(II)] complex.



Compound	X	Mesomorphism		
5	Cl	C 190 °C	N 205 °C	I
6	Br	C 210 °C	SmA 215 °C	N 250 °C I
7	I	C 220 °C	SmA 230 °C	I

Scheme 8. Phase transitions of a selected series of halo-bridged dinuclear azobenzene Pd(II) complexes.

mesomorphic properties, a series of dinuclear cyclopalladated complexes was synthesized, starting from the nematic symmetrically substituted azobenzene ligand **8** (Scheme 9) [28,29]. The chloro-bridged derivative **9** showed an interesting mesomorphic behaviour upon heating, with the unusual phase sequence: highly ordered crystalline C phase–disordered N phase–ordered SmE mesophase–isotropic liquid I, which is related to intermolecular forces coupled with structural modifications of the mesogenic species. In fact, in the crystalline solid state molecules of **9** are organized in pairs, with non-bonding Pd...Pd intermolecular separation of 3.67 Å while, as evidenced by PXRD measurements at variable temperature, within the layers of the SmE mesophase the average intermolecular distance is 4.0 Å. These data suggested that during the heating cycle the reversible $N \rightleftharpoons \text{SmE}$ transition was coupled to a reversible transformation from pairs of molecules present in the crystalline state, which are also present in the nematic phase, to a uniform array of single molecules within the SmE phase. PXRD measurements at a constant temperature and with different acquisition times proved that the nematic phase is not in thermodynamic equilib-



Compound	X	Mesomorphism		
8		C 108 °C	N 116 °C	I
9	Cl	C 213 °C	N 221 °C	SmE 235 °C I _{dec.}
10	Br	C 215 °C	I	
11	I	C 211 °C	I	

Scheme 9. Mesomorphism of 4,4'-bis(hexyloxy)azobenzene and of its halo-bridged dinuclear Pd(II) derivatives.

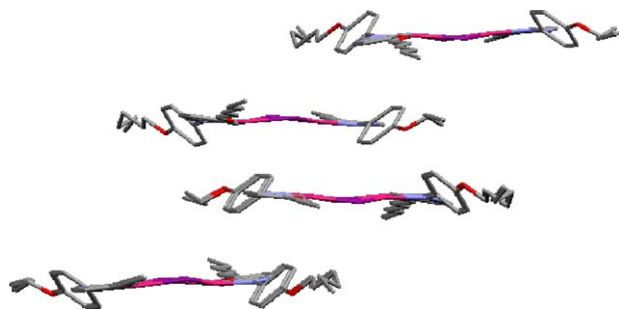
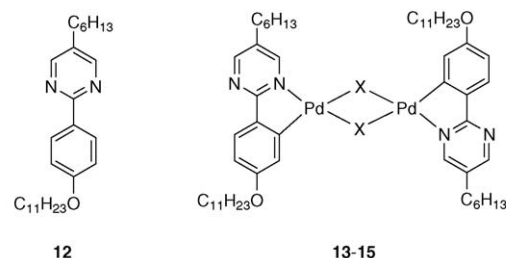


Fig. 6. Crystal packing of the dinuclear bromo-bridged 4,4'-bis(hexyloxy)azobenzene Pd(II) complex (**10**) showing the existence of association of molecules in dimers.

rium and, when subjected to an annealing process, transforms into a smectic phase. The ability of these complexes to organize into dimers in the crystal packing with intermolecular Pd...Pd distances in the 3.67–3.76 Å range, depending on the halogen bridged ligand, can be considered a consequence of the presence of a flat rigid central fragment, involving fused rings formed by the palladacycles, the palladated phenyl rings and the central Pd₂X₂ ring, which drives the entire molecule towards strong intermolecular core–core interactions (e.g., crystal packing of complex **10** showing the dimers organization; Fig. 6). In addition, the increase of the transition temperatures, the appearance of more ordered mesophases and, in some cases, the lack of mesomorphism with respect to the unmetalated ligands can be attributed to strong intermolecular interactions promoted by the presence of partially aromatic cyclopalladated rings.

A comparative photophysical study was performed in order to check the effects exerted by the different bridging groups on the spectroscopic properties of the homologous series of complexes [(C,N)Pd(μ-X)]₂ (HC,N = p,p'-bis(hexyloxy) azobenzene, **8**; X = halide, **9–11**; azido; thiocyanato; oxalato; acetato) [29]. All the complexes exhibited two broad band systems in the violet–visible wavelength region. The higher energy bands fall in the 370–380 nm range and compare well with the intense higher energy band displayed by the parent ligand **8** [29] at 360 nm. On these basis, for the whole set of [(C,N)Pd(μ-X)]₂ complexes the band around 370–380 nm is assigned to an intraligand ππ* transition. The quite intense band detected around 470 nm (ε > 10⁴ M⁻¹ cm⁻¹), which determines the colour of the complexes, is not present in the spectrum of azobenzene, where only a very weak band (ε ≅ 10³ M⁻¹ cm⁻¹) at 441 nm can be observed. The lower energy band is associated to a transition involving the cyclopalladated ring [30], with orbitals perturbed by the hexyloxy substituent of the metalated phenyl group. In addition, in contrast to the spectra of the other homologous complexes, the absorption spectrum of the complex with X = AcO shows a long tail on the red side of the lowest energy band, at about 520 nm. However, the molecular structure of such a complex is bent, with the two azobenzene moieties kept at a close distance by the acetato bridge and with a Pd...Pd separation of about 3 Å [31]. This geometry is believed to induce a high degree of interaction between the aromatic rings [32], which could be responsible for the mentioned shoulder. In complexes **9–11**, the state associated with the previously mentioned intraligand ππ*



Compound	X	Mesomorphism		
12		C 48 °C	N 59 °C	I
13	Cl	C 172 °C	SmA 219 °C	I
14	Br	C 171 °C	SmA 202 °C	I
15	I	C 149 °C	SmA 193 °C	I

Scheme 10. Mesomorphic behaviour of 5-(1-hexyl)-2-(4'-undecyloxy)phenylpyrimidine and of the corresponding cyclopalladated halo-bridged derivatives.

transition is slightly lowered in energy with respect to the deactivating metal centred states, inducing a weak luminescence (emission quantum yield ranging from 0.009 to 0.46%) in the 520–580 nm range.

Dinuclear cyclopalladated liquid crystals were also obtained from 5,4'-disubstituted-2-phenylpyrimidines, nematogenic ligands which can be metallated on the phenyl ring [33]. These species are mesogenic for X = Cl, Br or I, with mesomorphism and transition temperatures that confirm the trend observed for the analogous azobenzene complexes (Scheme 10), while the rigid roof-shaped geometry imposed by the AcO-bridge (e.g., X-ray structure of {(5-(1-hexyl)-2-[(4'-methoxy)phenyl-2'-ato]pyrimidine-N',C^{2'})-μ-acetato}dipalladium(II); Fig. 7) generates an overall non-planar structure preventing any mesomorphism [33].

The “H” shaped molecular structure, required for the [(C,N)Pd(μ-X)]₂ complexes to display thermotropic mesomorphism, originates from four lateral aliphatic chains placed at the p,p'-positions of the HC,N ligand. Since liquid–crystalline chiral phases are important materials for electrooptical devices, the p,p'-positions seem the obvious choice to introduce stereogenic centres. By using azobenzenes bearing stereogenic groups in the peripheral tails [34], the preparation of materials which retain the chiral phases of the organic precursors is easily accessible (Scheme 11).

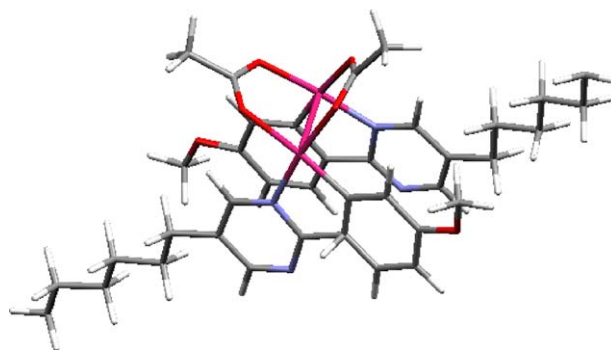
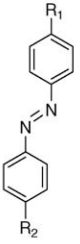
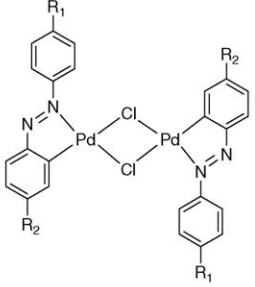


Fig. 7. Roof-shaped molecular structure of {(5-(1-hexyl)-2-[(4'-methoxy)phenyl-2'-ato]pyrimidine-N',C^{2'})-μ-acetato}dipalladium(II) complex.



16-17



18-19

Compound	R_1	R_2	Mesomorphism
16	S(-)- β -citronellyl ^a	OC ₇ H ₁₅	C 51 °C N* 66 °C I
17	S(-)- β -citronellyl ^a	OC ₁₂ H ₂₅	C 63 °C SmA* 69 °C I
18	S(-)- β -citronellyl ^a	OC ₇ H ₁₅	C 163 °C SmC* 176 °C I
19	S(-)- β -citronellyl ^a	OC ₁₂ H ₂₅	C 144 °C SmA* 164 °C I

^a S(-)- β -citronellyl = O(CH₂)₂CH(CH₃)(CH₂)CH=C(CH₃)

Scheme 11. Phase transitions of some chiral azobenzene ligands and their chloro-bridged dinuclear Pd(II) derivatives.

A further important family of cyclopalladated mesogens which is worth mentioning in this context is obtained from imines. In particular, in the accurate and elegant work carried out with these compounds mainly by Espinet and Serrano, the control of the mesomorphic properties and the induction of ferroelectricity and NLO properties was demonstrated. However, cyclopalladated imine complexes have been extensively reviewed elsewhere [1b] and therefore they are not included in the present account.

4.2. Mononuclear (C,N)Pd(O,N)

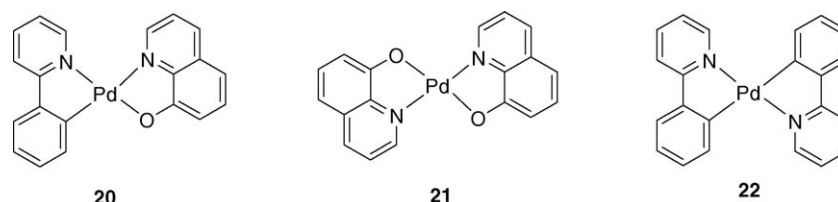
Mononuclear neutral (C,N)PdLX, (C,N)Pd(O,N) or (C,N)Pd(O,O) complexes, can be obtained in a simple way, starting from the dinuclear [(C,N)Pd(μ -X)]₂ species, by bridge splitting reactions with monodentate (L) or monoanionic chelating ligands (e.g., O,N or O,O).

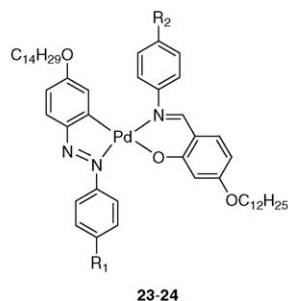
The structure of the (C,N)Pd(O,N) complexes consists of two different chelated ligands, with an asymmetric palladium coordination sphere that can be, in principle very important for photophysical properties. An interesting example [35] is given by complex **20** shown in Scheme 12, which emits in solution at room temperature at 540 nm, with a 0.60% quantum yield. The emission is confirmed by the excitation spectrum closely matching the corresponding absorption spectrum.

While the metalated complexes of the d⁸ ruthenium(II), osmium(II), platinum(II) and iridium(III) transition metals

exhibit luminescence at room temperature, the homologous palladium(II) species, excluding few examples [30,36–39], are known to emit only at low temperatures [40–42]. The metal centred (MC) states of palladium(II) complexes lie at lower energies than the ligand centred (LC) or metal to ligand charge transfer (MLCT) states, which is detrimental for luminescence efficiency. In fact, if the emitting (either LC or MLCT) and the MC states are too close in energy, they can thermally equilibrate, thereby quenching the emission through fast radiationless decay throughout the MC states. The energy gap between the MC states and the lowest energy emitting excited state may then be considered to be one of the limiting factors for emission efficiency (i.e., a small energy gap between emitting and MC states leads to poor emission efficiency). The room temperature emission quantum yield of **20** is low, but it is nevertheless interesting to note that the homoleptic complexes **21** and **22** [40] (Scheme 12) are reported to emit only at 77 K [43]. As suggested by the results of studies regarding similar heteroleptic compounds [44,45], it seems reasonable to propose that a quinolate centred state (mixed with a metal-localized state perturbed by the phenylpyridinate ligand) is involved in the deactivating radiative path of **20**. The energy gap between this LC state and the deactivating MC states in **20** is higher than in complexes **21** and **22** and the appearance of luminescence is then possible.

The possibility of inserting aliphatic chains at the periphery of the (C,N)Pd(O,N) core shared by this class of complexes, can be exploited in order to obtain materials with a non-crystalline

Scheme 12. Room temperature emitting heteroleptic cyclopalladated complex (**20**) and related homoleptic (**21** and **22**) Pd(II) species.



Compound	R_1	R_2	Mesomorphism			
23	S(-)- β -citronellyl ^a	C ₈ H ₁₇	C 85 °C	SmC* 90 °C	SmA* 100 °C	I
24	S(-)- β -citronellyl ^a	S(-)- β -citronellyl ^a	C 67 °C	SmC* 77 °C	N* 83 °C	I

^a S(-)- β -citronellyl = O(CH₂)₂CH(CH₃)(CH₂)CH=C(CH₃)

Scheme 13. Phase transitions of hetero-ligand cyclopalladated complexes containing chiral substituents on the aliphatic chains.

aggregation state. In particular, such an approach was fruitfully used for the preparation of new organopalladium thermotropic materials exhibiting, when compared to the corresponding halo-bridged dinuclear parents, lower transition temperatures and higher mesophases stability.

The developed strategy was based on the concept of non-symmetrical twin molecular arrangement: compounds formed by two different and independent mesogenic entities connected by one metal atom. Different classes of mixed-ligand cyclopalladated complexes were synthesized. From reaction of complex **9** with a series of salicylideneanilines or *o*-hydroxyazobenzenes the first examples of lateral–lateral fused organometallic mesogens were obtained [46,47]. These species, containing an asymmetric polar core, are nematogenic or smectogenic, with lower transition temperatures than those of the dinuclear complexes. The same approach was applied to prepare hetero-ligand complexes containing a cyclopalladated azo-moiety and a chelating resorcyldieneamine [48], which can be functionalized with chiral terminal tails. The advantage of this synthetic strategy was the possibility of readily performing modifications of the chemical nature of the substituents: several cyclopalladated complexes bearing a variable number of stereogenic centres in the lateral chains have been obtained, depending on the organic precursor selected. In addition, cyclopalladation induces a remarkable decrease in the clearing temperatures, when compared to the mesomorphic organic ligands, and promotes the appearance of smectic and/or nematic chiral phases also in complexes with non-mesomorphic azobenzene precursors (Scheme 13).

Practical applications in electrooptic devices usually require that the active materials have to be processed as transparent amorphous thin films. Species with four peripheral aliphatic chains can usually form amorphous or liquid crystalline films on heating or cooling. In other cases, as an alternative, homogeneous amorphous films can be obtained by rapidly cooling down the isotropic fluid or by solution in inert matrices (such as poly(vinyltoluene-co- α -methylstyrene), PVTMS, or poly(isobutyl methacrylate), PIBMA) of species with a molecular structure promoting and stabilizing a glassy state or

increasing miscibility in film forming polymers. Unfortunately, (C,N)Pd(O,N) cyclopalladated complexes without lateral substituents, as a general trend, exhibit high melting temperatures and poor miscibility in polymers. In addition, decompositions often occur while heating near melting temperatures. As a consequence, in order to avoid contamination, melting temperatures should be conveniently lowered and molecular shapes should be tailored to increase miscibility in host polymers. These properties can be conveniently induced if at least one aliphatic chain, bonded to the aromatic (C,N)Pd(O,N) core, is introduced.

A proper choice of ligands can lead to cyclopalladated complexes exhibiting mesomorphic properties. In particular, for complexes **23** and **24** (Scheme 13) the SmC* phase was observed. Because of its unique ferroelectric properties, the idea that the field reorienting the spontaneous polarization could also be a photogenerated space-charge field prompted the study of SmC* phases as media in which refractive index modulations can be optically controlled. This has been done by doping conventional materials with a small amount of photosensitizers to induce photoconduction and allow the set up of a photogenerated electric field. The cyclopalladated complexes **23** and **24** (Scheme 13) display instead photorefractivity without any doping [49]. Fig. 8 shows the asymmetric energy exchange when an aligned sample of **24** is illuminated with an interference pattern at $\lambda = 633$ nm, clearly indicating a photorefractive behaviour. Gain coefficients $\Gamma \sim 125 \text{ cm}^{-1}$ have been measured, well above what obtained for doped SmC* phases.

Some of the complexes for which adequate films formed (those arising from cyclometalated azobenzene or benzo[*h*]quinoline and an appropriate *p,p'*-salicylideneimine, **25** and **26**, respectively, Scheme 14) were found to display photoconducting properties (Fig. 9).

In addition, when photoconductivity is normalized to absorption coefficient and light intensity, cyclopalladated complexes, although not yet optimized in this respect, show a performance which is comparable with other common photoconductors such as polyvinylcarbazole (PVK). This is particularly

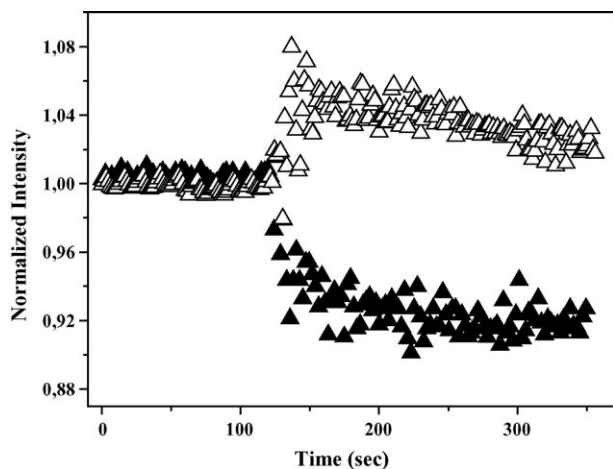


Fig. 8. Two-beam coupling in an aligned sample of **24**. At $t = 125$ s, an electric field $E = 5.4$ V/ μm was turned on.

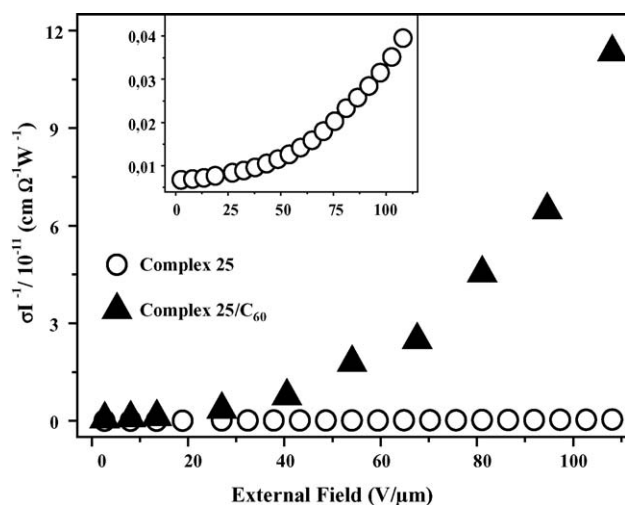


Fig. 9. Applied field dependence of the normalized photoconductivity at 633 nm for pure and C_{60} doped **25**. The inset shows the data for the pure sample on an enlarged scale with the same units.

evident from Fig. 9, where the field dependence of the photoconduction of **25** doped with C_{60} is illustrated. Photoconduction is increased by using dopants such as C_{60} , C_{70} or carbon nanotubes, which increase absorption and are known

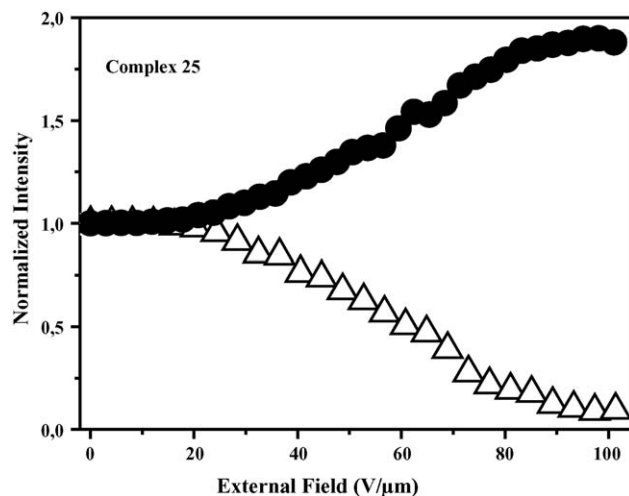
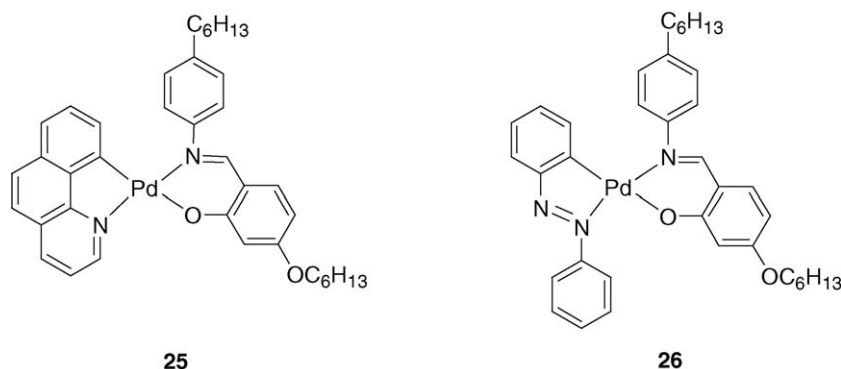


Fig. 10. Applied field dependence of two-beam coupling at 633 nm for **25**. It is evident how one of the beams gains the energy lost by the other one.

to stabilize electrons and thus promote hole formation. In the case of complex **25** we observe a normalized photoconduction $\sigma/(\alpha I) = 1.2 \times 10^{-12} \text{ cm}^2 \Omega^{-1} \text{ W}^{-1}$ at $\lambda = 633$ nm for an applied electric field $E = 100$ V/ μm , while for PVK doped with the dye Disperse Red 1 [50] $\sigma/(\alpha I) = 4.4 \times 10^{-13} \text{ cm}^2 \Omega^{-1} \text{ W}^{-1}$ at the same field. These results are encouraging and measurements are in progress to evaluate the different contributions of mobility and photogeneration efficiency.

The observation of photoconductivity in cyclopalladated complexes prompted the study of their photorefractive properties [51]. The first photorefractive materials were inorganic single crystals but more recently, due to their low cost, processability and ease of chemical modification, organic amorphous materials have attracted attention. The first evidence of photorefractive properties in cyclopalladated complexes was published a few years ago [52] and it soon became evident that their performance, when compared to other amorphous organics, was outstanding [53]. In Fig. 10, the asymmetric energy exchange between two coherent beams superimposing on a sample of complex **25** is illustrated.

This phenomenon, known as two-beam coupling, is related to the phase shift between the interference pattern of the two



Scheme 14. Examples of photorefractive cyclopalladated complexes.

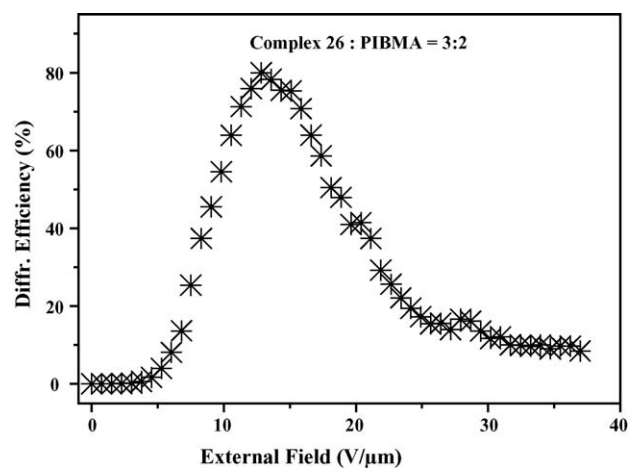


Fig. 11. Applied field dependence of the diffraction efficiency at 633 nm for a sample of complex **26** in PIBMA. The shape of the curve can be understood considering Eq. (3), which describes the dependence of the efficiency on the index modulation Δn . In our case, Δn increases with increasing applied field.

beams and the resulting index grating, and the effect can be quantified by a gain coefficient Γ . Observation of asymmetric energy exchange is then generally taken as the demonstration of photorefractive behaviour. It should be mentioned that the gain coefficient measured in these materials, $\Gamma = 750 \text{ cm}^{-1}$ at an applied field $E = 100 \text{ V}/\mu\text{m}$, is among the largest ever measured in amorphous organic materials. Another important parameter when evaluating photorefractive materials is the dynamic range, i.e., the Δn value that can be obtained. The dynamic range can be evaluated in four-wave mixing experiments, where the grating originating from a light interference pattern is “read” by a third light beam, which is diffracted. Within a first approximation, the

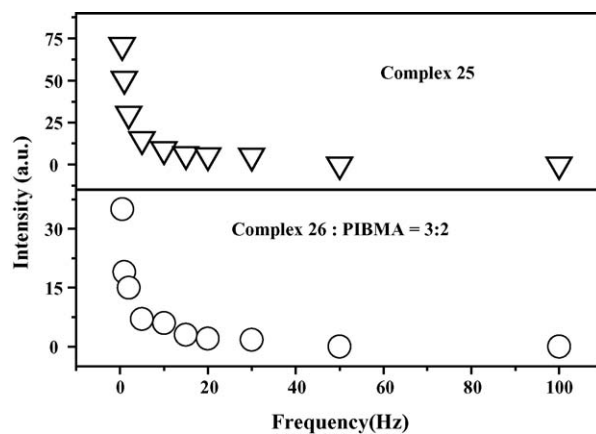


Fig. 12. Ellipsometric measurements for complexes **25** and **26**. In these experiments, samples are subjected to an ac electric field and the field-induced birefringence is recorded as a function of the frequency of the applied field.

diffraction efficiency η , defined as the percentage of diffracted light, is given by:

$$\eta \sim \sin^2 \left(\frac{\pi \Delta n d}{\lambda} \right) \quad (3)$$

where d is the thickness of a particular sample. Fig. 11 shows four-wave mixing results for a sample of complex **26** in a 3:2 mixture with PIBMA. Two features of these data should be underlined: the first overmodulation of the efficiency is obtained at a field $E \sim 11 \text{ V}/\mu\text{m}$ and the corresponding dynamic range is of the order of $\Delta n \sim 9 \times 10^{-3}$. In both cases, these values are among the best known to date for amorphous organic materials.

These excellent results motivated further studies [54] aimed at assessing the nature of the field-induced refractive index

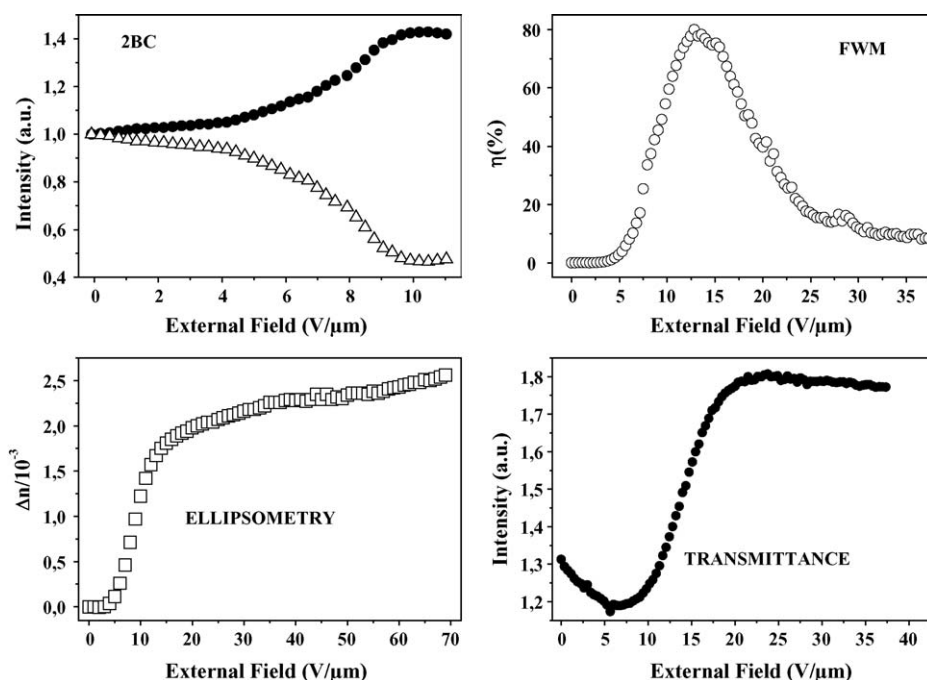


Fig. 13. Applied field dependence of beam intensities (two-beam coupling), diffraction efficiency (four-wave mixing), birefringence (ellipsometry) and light transmission in samples of complex **26** dissolved in PIBMA. In all cases, the field dependence becomes smaller at high fields.

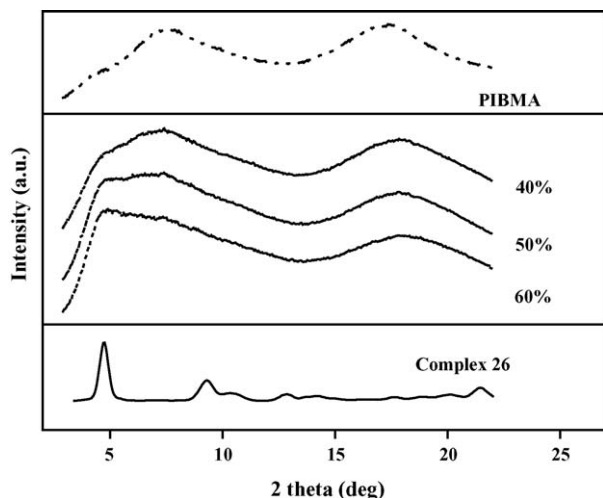


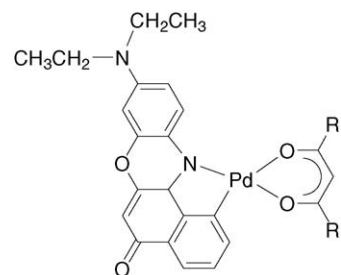
Fig. 14. X-rays diffraction patterns for complex **26**, PIBMA and mixtures of **26** in PIBMA at different concentrations. The crystalline nature of the dispersed complex is evident even for concentrations of **26** as low as 40%.

variations in amorphous phases of cyclopalladated complexes. In general, in organic materials the field can be effective via two different mechanisms: non-linear optical effects and reorientations of molecular dipoles. One of the main differences between the two mechanisms is that non-linear responses, being related to electron displacements, are much faster than molecular rotations: this fact can be used in ellipsometric experiments in which a biased ac field is applied on samples. If the frequency of the field is increased, the refractive index modulations at the field frequency due to molecular reorientations will disappear above a few tens or hundreds of Hertz while the modulations due to non-linear optical effects will still be present at much higher frequencies. These experiments are typically carried out by following the field-induced birefringence in samples acting as phase retarders between crossed polarizers. Fig. 12 shows results for samples of **25** and **26**: the response to the field disappears above 10–20 Hz, clearly indicating that in these systems only field induced reorientational mechanisms are active.

Further studies were conducted in order to investigate more in detail the nature of the reorientational process [55]. As shown in Fig. 13, samples in which the cyclopalladated complex **26** is dissolved in a polymer may show a field dependence of several properties indicating that a field induced reorientation is complete at fields of the order of 20 V/μm.

This fact is unusual and difficult to understand in terms of molecular reorientations, since for these fields the dipole (P)–field (E) interaction energy $F \sim PE$ is at least one order of magnitude lower than thermal energy $k_B T \sim 5 \times 10^{-21}$ J, even considering extremely large dipoles of the order of 10 Debyes. Given the relatively high concentration of the active cyclopalladated species present in these mixtures, the presence of crystalline aggregates was sought and confirmed by X-ray analysis, as shown in Fig. 14.

The size of the crystals is below 200–300 nm, as confirmed by scanning electronic spectroscopy (SEM) and atomic force microscopy (AFM) investigations and by the fact that samples



27–29

Compound	R	λ_{em}^a (nm)	Φ^a (%)
27	CH ₃	585, 638	12
28	CF ₃	595, 650	50
29	C ₆ H ₅	587, 636	14

^a cyclohexane solution

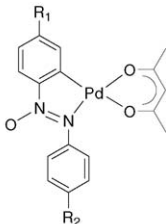
Scheme 15. Emitting properties of the cyclopalladated Nile Red fragment complexed to substituted acetylacetones.

appear clear and transparent both under the naked eye and upon optical microscope inspection. The presence of such crystalline domains can explain the high photorefractive performance of these materials at relatively low fields, since the reorientation mechanism is now different: not anymore interactions with the dipole of single molecules, but reorientations of whole nano-sized crystals due to their dielectric anisotropy $\Delta\epsilon$. In this case, the interaction energy F of crystals of volume V with the field E can be written as $F = (1/2)\epsilon_0 \Delta\epsilon E^2 V \gg k_B T$ even for small values of dielectric anisotropy. Cyclopalladated complexes were then the first class of photorefractive materials in which this innovative hybrid morphology consisting of dispersions of small crystals within an amorphous matrix was used to boost performance.

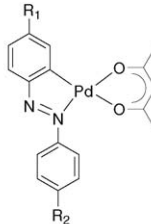
4.3. Mononuclear (C,N)Pd(O,O)

As previously mentioned, a straightforward route to obtain mononuclear species from dinuclear ones is the reaction of $[(C,N)Pd(\mu-X)]_2$ with (O,O) monoanionic bidentate ligands, such as acetylacetone or derivatives. In this class of complexes the palladium(II) ion is bonded to two chelated fragments which display very different electron donating properties, as it is clearly evident from the photophysical properties exhibited by the Nile Red (9-diethylamino-5H-benzo[*a*]phenoxazine-5-one) derivatives **27–29** (Scheme 15).

The absorption spectra of these complexes [56] are quite similar, with a series of bands attributable to the Nile Red ligand centred (LC) metal-perturbed transitions, and show a significant solvatochromism. Luminescence studies at room temperature evidence very interesting peculiarities. All complexes emit with a relevant intensity in a wide portion of the visible spectrum, showing emission bands associated with deactivation of Nile Red LC states slight mixed with the MC ones. The emission bands suffer a relevant solvatochromism: in **27**, for example, maxima range from 585 nm in cyclohexane to 712 nm in methanol [56]. The quantum yield (Φ) shows a striking depen-



30



31-34

Compound	R_1	R_2	Mesomorphism
30	OC ₆ H ₁₃	OC ₆ H ₁₃	C 90 °C N 105 °C I
31	<i>S</i> (-)- β -citronellyl	OC ₇ H ₁₅	C 47 °C N* 65 °C I
32	<i>S</i> (-)- β -citronellyl	OC ₁₂ H ₂₅	C 40 °C SmA* 63 °C I
33	R(-)-2-octyl ^b	OC ₇ H ₁₅	C 55 °C N* 58 °C I
34	R(-)-2-octyl ^b	OC ₁₄ H ₂₉	C 48 °C SmA* 61 °C I

^a *S*(-)- β -citronellyl = O(CH₂)₂CH(CH₃)(CH₂)CH=C(CH₃); ^b = OCH(CH₃)(CH₂)₅CH₃

Scheme 16. Mesomorphism of selected examples of acetylacetonato complexes of cyclopalladated chiral 4,4'-disubstituted-azobenzenes.

dence on solvent polarity: in the case of **28** an increase from 0.02 in methanol to 0.5 in cyclohexane is observed. This behaviour, evidenced in all examined complexes, can be attributed to the presence of a twisted intramolecular charge transfer (TICT) state [57–59] localized on the Nile Red moiety and with an energy comparable to the lowest energy LC state. The emission quantum yield of these complexes has been demonstrated to be tuned by the electronic effects exerted by the substituents placed on the acetylacetonato ligand [56]. In particular, the Φ value measured for **28** in cyclohexane was of 50%, which is, to the best of our knowledge, the highest reported to date for a palladium(II) complex. The tunability of the Φ value and the high emission intensity exhibited by these cyclopalladated Nile Red complexes are peculiar of the Nile Red ligand, and are preserved in the complexes because of the high energy gap between the emitting LC state and the MC state.

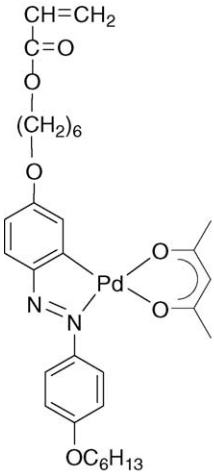
Palladium(II) acetylacetonato azobenzene complexes, although lacking in luminescence because of the $n\pi^*$ character of the azobenzene centred state [60], show interesting liquid crystalline properties. In this case, the asymmetric molecular structures disrupts the “H” molecular shape typical of other cyclopalladated rod-like complexes, hindering strong intermolecular interactions and inducing less ordered mesophases at lower temperatures [61,62]. The physical properties of complex **30** (Scheme 16) were extensively investigated [63] and exciting flexoelectric properties were found [64,65]. Liquid crystalline phases were also exhibited by nematogenic mononuclear complexes of three rings *p,p'*-azobenzenes containing anionic chelating ligands such as tropolone [66] as well as by acetylacetonato complexes based on azobenzenes bearing stereogenic centres in the alkoxy *p,p'*-chains [67], displaying low temperature chiral mesophases (**31–34**; Scheme 16).

(C,N)Pd(O,O) complexes have also been successfully tested as monomers for the synthesis of polymeric liquid crystalline organometallic materials: by polymerization of **35** [68], the homopolymer **36** (Scheme 17) was prepared. Laser induced per-

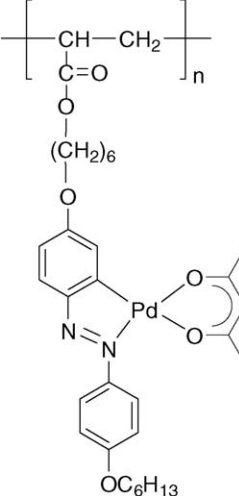
manent gratings could be written in films of **36**, suggesting its use as a material for optical storage [69].

4.4. Mononuclear (C,N)Pd(N,N)

The reaction between the cyclopalladated chloro-bridged dinuclear complex of 5-(1-hexyl)-2-[(4'-undecyloxy)phenyl]pyrimidine and the neutral chelating ligand 2,2'-bipyridine, forms the nematogenic complex **37** (Scheme 18). Complex **37** was the first example of a cyclometallated ionic mesogen and led the way to the synthesis of a new class of ionic thermotropic liquid crystals [61]. The counter-ion plays an important tuning role on the



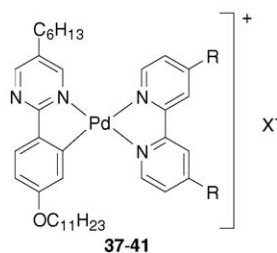
35



36

Compound	Mesomorphism
35	C 59 °C SmA 62 °C N I
36	C 48 °C Tg 115 °C I

Scheme 17. Mesomorphism of a cyclopalladated monomer and of its polymer.



Compound	R	X	Mesomorphism
37	H	BF ₄	C 146 °C N 158 °C I
38	COOC ₂₂ H ₄₅	BF ₄	C 83 °C SmC 146 °C I
39	CH ₂ OH	BF ₄	C 50 °C SmC 149 °C I
40	COOC ₂₂ H ₄₅	ClO ₄	C 205 °C SmA 235 °C I _{dec.}
41	CH ₂ OH	ClO ₄	C 210 °C SmA 212 °C I _{dec.}

Scheme 18. Mesomorphism of ionic phenylpyrimidine cyclopalladated complexes.

liquid crystalline properties of these species. In fact, a nematic mesophase was formed only by the tetrafluoroborate derivative, while no mesomorphism was observed with other anions.

The recent availability of an easy synthetic route to 4,4'-disubstituted-2,2'-bipyridines, allowed investigations of the thermotropic liquid crystalline behaviour of ionic cyclopalladated complexes with molecular shapes at the calamitic/discotic cross-over point. A further class of ionic orthopalladated complexes has then been obtained by the combination of the usual calamitic phenylpyrimidine ligand with half-disk non-mesogenic 4,4'-disubstituted-2,2'-bipyridines. Interestingly, the molecular geometry of complexes **38–41** (Scheme 18), induced a lamellar mesomorphism, namely a SmA or SmC phase, whatever the counter-ion or the lateral substituent [70].

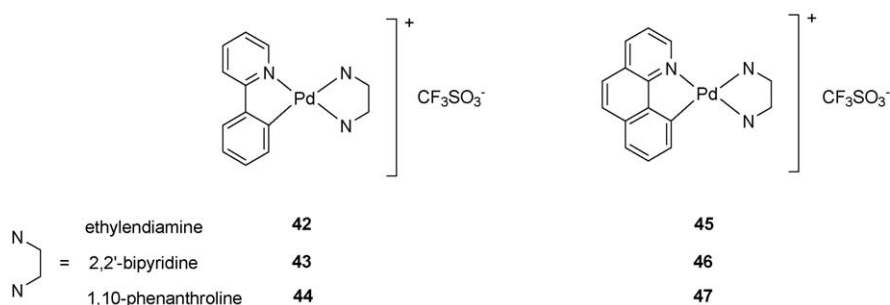
A series of photophysical studies were conducted on similar cyclometalated Pd(II) asymmetric complexes with an N,N ancillary ligand [45,71,72]. Results suggest that the electronic transitions are mostly ligand-localized, as the frontier orbitals are almost unaffected by the metal orbitals. This hypothesis was tested for the two homologous series, **42–44** and **45–47** (Scheme 19), and although the low solubility prevented a systematic study, photophysical data evidenced no appreciable solvatochromic effect, implying that electronic transitions do not have a significant charge transfer character. These results, together with cyclovoltammetric measurements, agree with the localization of the frontier orbitals on the cyclometalated moiety [73].

5. Conclusions and perspectives

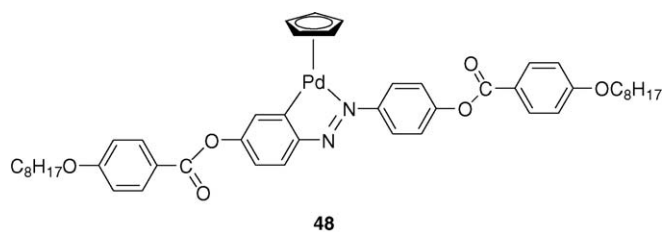
5.1. Synthesis of new species with improved performances

The formation of cyclopalladated complexes is an extensively reviewed subject and considering both their synthesis and stability, the best results are obtained when a planar five-membered ring is formed. The products separating from the reaction mixture when the selected HC,N ligand undergoes the cyclopalladation process, are X-bridged dinuclear complexes [(C,N)Pd(μ-X)]₂ (X = Cl or AcO). These compounds are useful reagents for the preparation of different classes of mononuclear complexes with physical properties suitable for practical applications. Important results on the relationships between molecular structure and thermotropic or luminescence properties could be derived from the body of synthetic work carried out to prepare new molecular materials.

Mesogenic properties, with phases ranging from nematic to lamellar and discotic, were indeed found to depend on the metal coordination geometry, on the number and length of flexible chains and on the core length/breadth ratio. Thermal behaviour is strongly affected by molecular shape and by the anisotropy of intermolecular forces: as the complexes symmetry lowers, so do the transition temperatures. For example, a variation of the planar geometry of azobenzene complexes (e.g., **48**; Scheme 20) due to the inclusion of a cyclopentadienyl group in the metal coordination sphere, induced a nematic phase, a substantial low-



Scheme 19. Examples of cyclopalladated ionic complexes with N,N' chelating ligands.



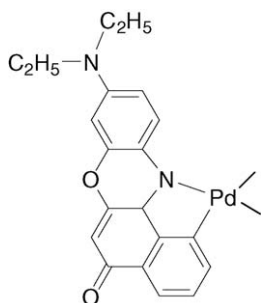
Scheme 20. Representative example of a mesogenic cyclopalladated complex with a non-planar lateral ligand.

ering of the clearing point and the suppression of the smectic phase [74].

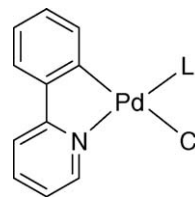
Red luminescent materials, with the highest emission quantum yields reported to date for a palladium(II) complex, have been obtained with complexes formed by the Nile Red cyclopalladated moiety (Scheme 21) and ancillary ligands such as acetylacetonato-like species, 27–29. The Nile Red emitting features are preserved as the dye ligand centred state is the lowest in energy.

The investigations summarized in the present account are focused on the preparation of molecular materials and the results of preliminary studies performed to elucidate their physical properties suggest that these palladium containing complexes are very useful photoactive species with liquid crystalline, luminescent or photorefractive properties. On the basis of these results, it is now possible to design new molecules which, together with the desired mesomorphism, can display different functionalities such as chirality, luminescence or photorefractivity.

The unique combination of anisotropic physical properties induced by molecular order with liquid-like viscosity has made a variety of applications possible. An example is given by the technologies centred on liquid crystals, currently extensively used in displays and as ideal active components in many molecular electronics and photonics devices such as waveguides and light modulators. At this stage, the target of chemical research is the design of novel types of mesogenic materials that can widen the present technologies, possibly combining different functionalities. By exploiting well-tested synthetic protocols, syntheses of materials with improved performances or tailored for specific applications may be within reach.



Scheme 21. The cyclopalladated Nile Red synthon.



Scheme 22. General formula of 2-phenylpyridine Pd(II) derivatives, where L can be an aromatic or an aliphatic amine ligand.

5.2. Further applications

The (C,N)Pd(O,N) cyclopalladated complexes with a variety of ligands have shown excellent photoconductive properties in amorphous glassy films as pure materials and measurements of charge carriers mobility are in progress. Electrochemical studies of the synthesized derivatives by cyclic voltammetry and the correlated theoretical energy level calculations have also been performed. Both experimental and theoretical data show that the energy levels of the frontier orbitals (HOMO–LUMO) are separated in space by the metal centre. The LUMO energy level is determined by the nature of the cyclometalated ligand (between 2.6 and 4.0 eV), whereas the HOMO energy level is invariably placed at $E_{\text{HOMO}} \sim 5.8$ eV, with a charge density mainly distributed on the auxiliary ligand. This peculiarly separated HOMO–LUMO charge density distribution could therefore be at the origin of the photoconductive and, ultimately, of the photorefractive properties of this class of compounds. In this respect, further experimental and theoretical studies regarding the first excited electronic states are necessary in order to clarify the nature of the photogeneration processes. An optimization of photogeneration is, in fact, important because could open the way to applications of cyclopalladated complexes in new fields, as those related to solar energy conversion.

Moreover, considering the biological applications of cyclopalladated species, the results of some preliminary biological studies performed on new cyclopalladated complexes containing acridine ligands open the way to pharmacological uses and further enlarge the gamut of possible applications for cyclopalladated complexes. Cyclometalated compounds were shown to be particularly interesting in antitumor research. Many examples, with different types of ligands and metals including palladium(II) and platinum(II) benzylidenamines [75], platinum(II) terpyridine [76], gold(III) [77] and platinum(II) 2-phenylpyridine [78,79], palladium(II) and platinum(II) thiosemicarbazones [80], palladium(II) azobenzene [81,82] show cytotoxic effects against various tumor cells. Compared to their platinum(II) analogues, cyclopalladated complexes are more stable and, most important, being less toxic, they have a more specific antitumor activity in vitro [83]. Some mononuclear complexes based on cyclopalladated 2-phenylpyridine, containing as labile ligand an aromatic or aliphatic amine (Scheme 22), tested against a panel of seven tumor cell lines, have been found to be cytotoxic [84].

In perspective, the results obtained with the reported studies suggest that the chemistry of cyclopalladated complexes can have relevant implications not only in the solid state, as amor-

phous films of photoconducting materials, but in solution as well, for the preparation of bioactive molecules. Therefore, either as advanced materials or as molecules for pharmacological uses, cyclopalladated complexes still present intriguing opportunities for further explorations.

Acknowledgements

The work described in this review was supported by the Università della Calabria, by the Italian Ministero dell'Università e della Ricerca (CIPE L. 488/92: Cluster 14, S.P. 5 and Cluster 26, S.P. 8; INSTM-FIRB-2001 and Centro di Eccellenza CEMIF.CAL grants) and by the European Commission (Marie Curie development host fellowship Contract HPMD-CT-2002-00073) to whom we are grateful. We also thank Dr. Davide Dattilo, Dr. Roberto Termine, Dr. Mara Talarico, Dr. Teresa Pugliese, Dr. Nicolas Godbert, Dr. Giovanna Barberio, Dr. Rossana Bloise and the many graduate students who, during the time, have contributed to this work.

References

- [1] (a) J. Dupont, C.S. Consorti, J. Spencer, *Chem. Rev.* 105 (2005) 2527, and references therein;
(b) B. Donnio, D. Guillon, R. Deschenaux, D.W. Bruce, in: J.A. McCleverty, T.J. Meyer (Eds.), *Comprehensive Coordination Chemistry II*, vol. 6, Elsevier, Oxford, 2003.
- [2] H. Takahashi, J. Tsuji, *J. Organomet. Chem.* 10 (1965) 511.
- [3] J. Dupont, M. Pfeffer, J. Spencer, *Eur. J. Inorg. Chem.* (2001) 1917.
- [4] I. Omae, *Coord. Chem. Rev.* 248 (2004) 995.
- [5] I.P. Beletskaya, A.V. Cheprakov, *J. Organomet. Chem.* 689 (2004) 4055.
- [6] M. Ohff, A. Ohff, D. Milstein, *Chem. Commun.* (1999) 357.
- [7] B. Crociani, T. Boschi, R. Pietropaolo, U. Bellucco, *J. Chem. Soc. A* (1970) 531.
- [8] J. Albert, R. Bosque, J. Granell, R. Tavera, *Polyhedron* 20 (2000) 3225.
- [9] J. Albert, M. Gomèz, J. Granell, J. Sales, *Organometallics* 9 (1990) 1405.
- [10] J. Albert, R.M. Ceder, M. Gomèz, J. Granell, J. Sales, *Organometallics* 11 (1992) 1536.
- [11] C. Navarro-Ranninger, I. López-Solera, A. Alvarez-Valdés, J.H. Rodríguez-Ramos, J.R. Masaguer, J.L. García-Ruano, *Organometallics* 12 (1993) 4104.
- [12] M. Calvin, K.W. Wilson, *J. Am. Chem. Soc.* 67 (1945) 2003.
- [13] H. Masui, *Coord. Chem. Rev.* 219 (2001) 957.
- [14] A. Crispini, M. Ghedini, *J. Chem. Soc., Dalton Trans.* (1997) 75.
- [15] R.M. Ceder, M. Gomez, J. Sales, *J. Organomet. Chem.* 361 (1989) 391.
- [16] A. Castiñeiras, A.G. Sicilia-Zafra, J.M. González-Pérez, D. Choquesillo-Lazarte, J. Niclòs-Gutiérrez, *Inorg. Chem.* 41 (2002) 6956.
- [17] M. Ghedini, I. Aiello, A. Crispini, M. La Deda, *Dalton Trans.* (2004) 1386.
- [18] J.W. Goodby, in: D. Demus, J.W. Goodby, G.W. Gray, H.-W. Spiess, V. Vill (Eds.), *Handbook in Liquid Crystals*, vol. 2A, Wiley-VCH, Weinheim, 1999 (Chapter 1).
- [19] J. Mort, D.M. Pai (Eds.), *Photoconductivity and Related Phenomena*, Elsevier, Amsterdam, 1976.
- [20] J.S. Schildkraut, A.V. Buettner, *J. Appl. Phys.* 72 (1992) 1888.
- [21] J.S. Schildkraut, Y. Cui, *J. Appl. Phys.* 72 (1992) 5055.
- [22] P. Günter (Ed.), *Nonlinear Optical Effects and Materials*, Springer, Berlin, 2000 (Chapter 4).
- [23] H. Kelker, R. Hatz, *Handbook of Liquid Crystals*, Verlag Chemie, Weinheim, 1980.
- [24] M. Ghedini, M. Longeri, R. Bartolino, *Mol. Cryst. Liq. Cryst.* 84 (1982) 207.
- [25] A.M. Giroud-Godquin, P.M. Maitlis, *Angew. Chem. Int. Ed. Engl.* 30 (1991) 375.
- [26] S. Armentano, A. Crispini, G. De Munno, M. Ghedini, F. Neve, *Acta Cryst. C* 47 (1991) 2545.
- [27] M. Ghedini, S. Licoccia, S. Armentano, *Mol. Cryst. Liq. Cryst.* 108 (1984) 269.
- [28] A. Crispini, M. Ghedini, S. Morrone, D. Pucci, O. Francescangeli, *Liq. Cryst.* 20 (1996) 67.
- [29] M. Ghedini, D. Pucci, A. Crispini, I. Aiello, F. Barigelletti, A. Gessi, O. Francescangeli, *Appl. Organomet. Chem.* 13 (1999) 565.
- [30] M. Ghedini, D. Pucci, G. Calogero, F. Barigelletti, *Chem. Phys. Lett.* 267 (1997) 341.
- [31] J.L. Garcia-Ruano, I. Lopez-Solera, J.R. Masaguer, C. Navarro-Ranninger, J.H. Rodriguez, S. Martinez-Carraera, *Organometallics* 11 (1992) 3013.
- [32] V. Balzani, F. Scandola, *Supramolecular Photochemistry*, Ellis Horwood, Chichester, 1991 (Chapter 9).
- [33] M. Ghedini, D. Pucci, G. De Munno, D. Viterbo, F. Neve, S. Armentano, *Chem. Mater.* 3 (1991) 65.
- [34] M. Ghedini, D. Pucci, E. Cesarotti, P. Antogniazza, O. Francescangeli, R. Bartolino, *Chem. Mater.* 5 (1993) 883.
- [35] M. Ghedini, I. Aiello, M. La Deda, A. Grisolia, *Chem. Commun.* (2003) 2198.
- [36] Y. Wakatsuki, H. Yamazaki, P.A. Grutsch, M. Santhanam, C. Kutal, *J. Am. Chem. Soc.* 107 (1985) 8153.
- [37] B.C. Tzeng, S.C. Chan, M.C.W. Chan, C.M. Che, K.K. Cheung, S.M. Peng, *Inorg. Chem.* 40 (2001) 6699.
- [38] F. Neve, A. Crispini, C. Di Pietro, S. Campagna, *Organometallics* 21 (2002) 3511.
- [39] I. Aiello, M. Ghedini, M. La Deda, *J. Lumin.* 96 (2002) 249.
- [40] M. Maestri, D. Sandrini, V. Balzani, A. von Zelewsky, C. Deuschel-Cornioley, P. Joliet, *Helv. Chim. Acta* 71 (1988) 1053.
- [41] K.A. Van Houten, D.C. Heath, C.A. Barringer, A.L. Rheingold, R.S. Pilato, *Inorg. Chem.* 37 (1998) 4647.
- [42] D. Song, Q. Wu, A. Hook, I. Kozin, S. Wang, *Organometallics* 20 (2001) 4683.
- [43] H. Yersin, D. Donges, J.K. Nagle, R. Sitters, M. Glasbeek, *Inorg. Chem.* 39 (2000) 770.
- [44] J. Brooks, Y. Babayan, S. Lamansky, P.I. Djurovich, I. Tsyba, R. Bau, M.E. Thompson, *Inorg. Chem.* 41 (2002) 3055.
- [45] T. Pugliese, N. Godbert, M. La Deda, I. Aiello, M. Ghedini, *Chem. Phys. Lett.* 410 (2005) 201.
- [46] M. Ghedini, S. Morrone, O. Francescangeli, R. Bartolino, *Chem. Mater.* 4 (1992) 1119.
- [47] M. Ghedini, S. Morrone, O. Francescangeli, R. Bartolino, *Chem. Mater.* 6 (1994) 1971.
- [48] D. Pucci, O. Francescangeli, M. Ghedini, *Mol. Cryst. Liq. Cryst.* 372 (2001) 51.
- [49] M. Talarico, G. Barberio, D. Pucci, M. Ghedini, A. Golemme, *Adv. Mater.* 15 (2003) 1374.
- [50] B. Kippelen, K. Meerholz, N. Peyghambarian, in: H.S. Nalwa, S. Miyata (Eds.), *Nonlinear Optics of Organic Molecules Polymers*, CRC Press, Boca Raton, 1997 (Chapter 8).
- [51] L. Solymar, D.J. Webb, A. Grunnet-Jepsen, *The Physics Applications of Photorefractive Materials*, Clarendon, Oxford, 1996.
- [52] I. Aiello, D. Dattilo, M. Ghedini, A. Golemme, *J. Am. Chem. Soc.* 123 (2001) 5598.
- [53] I. Aiello, D. Dattilo, M. Ghedini, A. Bruno, R. Termine, A. Golemme, *Adv. Mater.* 14 (2002) 1233.
- [54] A. Golemme, I. Aiello, D. Dattilo, D. Pucci, M. Ghedini, M. Talarico, R. Termine, *Proc. SPIE* 5521 (2004) 103.
- [55] R. Termine, I. Aiello, D. Dattilo, M. Ghedini, A. Golemme, *Adv. Mater.* 15 (2003) 723.
- [56] M. La Deda, M. Ghedini, I. Aiello, T. Pugliese, F. Barigelletti, G. Accorsi, *J. Organomet. Chem.* 690 (2005) 857.
- [57] W. Rettig, *Angew. Chem. Int. Ed. Engl.* 25 (1986) 971.
- [58] K. Bhattacharyya, M. Chowdhury, *Chem. Rev.* 93 (1993) 507.

- [59] P. Hazra, D. Chakrabarty, A. Chakraborty, N. Sarkar, *Chem. Phys. Lett.* 388 (2004) 150.
- [60] H. Rau, in: H. Durr, H. Bouas-Laurent (Eds.), *Photochromism*, Elsevier, Amsterdam, 1990.
- [61] M. Ghedini, D. Pucci, *J. Organomet. Chem.* 395 (1990) 105.
- [62] C. Versace, V. Formoso, D. Lucchetta, D. Pucci, C. Ferrero, M. Ghedini, R. Bartolino, *J. Chem. Phys.* 98 (1993) 8507.
- [63] O. Francescangeli, C. Ferrero, D. Pucci, M. Ghedini, *Mol. Cryst. Liq. Cryst.* 378 (2002) 77, and references therein.
- [64] A.Th. Ionescu, D. Pucci, N. Scaramazza, C. Versace, A.G. Petrov, R. Bartolino, *J. Chem. Phys.* 103 (1995) 5144.
- [65] A.G. Petrov, A.Th. Ionescu, C. Versace, N. Scaramuzza, *Liq. Cryst.* 19 (1995) 169.
- [66] M. Ghedini, S. Morrone, F. Neve, D. Pucci, *Gazz. Chim. Ital.* 126 (1996) 511.
- [67] M. Ghedini, D. Pucci, E. Cesarotti, O. Francescangeli, R. Bartolino, *Liq. Cryst.* 16 (1994) 373.
- [68] M. Ghedini, I. Aiello, A. Roviello, *Acta Polym.* 48 (1997) 400.
- [69] G. Cipparrone, A. Mazzulla, I. Aiello, M. Ghedini, *Mol. Cryst. Liq. Cryst.* 320 (1998) 165.
- [70] D. Pucci, G. Barberio, A. Bellusci, A. Crispini, M. Ghedini, *J. Organomet. Chem.*, 2006, in press.
- [71] F. Barigelletti, D. Sandrini, M. Maestri, V. Balzani, A. von Zelewsky, L. Chassot, P. Jolliet, U. Maeder, *Inorg. Chem.* 27 (1988) 3644.
- [72] K.A. Van Houten, D.C. Heath, C.A. Barringer, A.L. Rheingold, R.S. Pilato, *Inorg. Chem.* 37 (1998) 4647.
- [73] T. Pugliese, N. Godbert, M. La Deda, I. Aiello, M. Ghedini, *Inorg. Chem. Commun.* 9 (2006) 93.
- [74] M. Ghedini, D. Pucci, F. Neve, *Chem. Commun.* (1996) 137.
- [75] C. Navarro-Ranninger, J. Lopez-Solera, V.M. Gonzales, J.M. Perez, A. Alvarez-Valdes, P.R. Raithby, J.R. Masanger, C. Alonso, *J. Med. Chem.* 35 (1996) 5181.
- [76] D.L. Ma, C.M. Che, *Chem. Eur. J.* 9 (2003) 6133.
- [77] D. Fan, C.T. Yang, J.D. Ranford, P.F. Lee, J.J. Vittal, *Dalton Trans.* (2003) 2680.
- [78] C.M. Che, M. Yang, K.H. Wong, H.L. Chang, W. Lam, *Chem. Eur. J.* 5 (1999) 3350.
- [79] T. Okada, I.M. El-Mehasseb, M. Kodaka, T. Tomohiro, K. Okamoto, H. Okuno, *J. Med. Chem.* 44 (2001) 4661.
- [80] A.G. Quiroga, C.N. Ranninger, *Coord. Chem. Rev.* 248 (2004) 119.
- [81] M. Curic, L. Tusek-Bozic, D. Vikić-Topić, V. Scarica, A. Furlani, J. Balzarini, E. De Clercq, *J. Inorg. Biochem.* 63 (1996) 125.
- [82] L. Tusek-Bozic, M. Homac, M. Curic, A. Lycka, M. D'alpeos, V. Scarica, A. Furlani, *Polyhedron* 19 (2000) 937.
- [83] E.G. Rodriguez, L.S. Silva, D.M. Fausto, M.S. Hayashi, S. Dreher, E.L. Santos, J.B. Pesquero, L.R. Travessos, A.C.F. Caires, *Int. J. Cancer* 107 (2003) 498.
- [84] J.D. Higgins III, L. Neely, S. Fricker, *J. Inorg. Biochem.* 49 (1993) 149.